Basket scales of the green alga, *Mesostigma viride*: chemistry and ultrastructure

DAVID S. DOMOZYCH*

Department of Biology, Skidmore College, Saratoga Springs, NY 12866, USA

BRIAN WELLS and PETER J. SHAW

Department of Cell Biology, John Innes Institute for Plant Science Research, Colney Lane, Norwich NR4 7UH, UK

* Author for correspondence

Summary

The unicellular green algal flagellate, *Mesostigma viride*, possesses an extracellular matrix consisting of three layers of highly distinct scales. This study focused upon the elaborate basket scales. The basket scale is approximately 450–500 nm in height and consists of a solid base, two distinct lattices, two upper rims and various struts and roots. Pure preparations of isolated basket scales were obtained and used for subsequent chemical and immunological analyses. X-ray microanalyses revealed the scale as being mineralized with both calcium and phosphorus. Fourier Transform Infrared Spectroscopic analyses revealed the presence of phosphate, suggesting in turn that the basket scale is complexed with calcium phosphate. SDS–gel electrophoresis of partially digested scales revealed the presence of two protein components, a high M_r, non-migrating form and a form with a M_r of approximately 48 000. Further biochemical analyses of scales showed the presence of two major sugars: glucose and the unusual keto sugar acid, 3-deoxy-lyxo-2-heptulosaric acid, or DHA. Antibodies to scales were raised in rats and used in immunolabeling studies. It is estimated from immunofluorescence studies that a cell of 8 μm contains about 800 basket scales. The scales are in a close-packed arrangement resulting in quasi-crystalline arrays upon the cell surface.

Key words: basket scales, extracellular matrix, *Mesostigma*, DHA, calcium phosphate.

Introduction

The extracellular matrices of green plants constitute a heterogeneous assortment of biochemicals and complexed minerals. Modern research efforts have shown that these coverings range from the polysaccharide/glycoprotein-based cell wall meshwork of higher plants, to crystalline glycoprotein walls of chlamydomonad flagellates, to mineralized coverings of green algae (Roberts, 1989; Roberts *et al.* 1985; Adair and Snell, 1990; Varner and Lin, 1989; Simkiss and Wilbur, 1989; Porcella and Walne, 1980). In addition to understanding the chemical nature and polymeric microarchitecture of plant cell coverings, recent research has just begun to focus upon elucidating the secretory pathways involved in the intracellular processing of plant extracellular matrices (Ali *et al.* 1986; Brummel *et al.* 1990; Moore *et al.* 1991; Moore and Staehelin, 1988; Staehelin and Chapman, 1987; Staehelin *et al.* 1990). In the most primitive, extant group of green plants, the Prasinophyceae or Micromonadophyceae (Mattox and Stewart, 1984; Norris, 1980), many organisms are characterized by a distinct extracellular covering of scales. The various scale types often possess elaborate morphology and are often arranged in multiple layers upon the cell and flagellar surfaces (Pennick, 1984; Domozych, 1989). In some genera, hundreds of thousands of scales may coat the surface of a single cell (e.g. see Moestrup and Walne, 1979). Electron-microscopic studies have revealed that the scales are processed within the Golgi apparatus (GA) (Manton, 1966; Manton and Ettl, 1965; for review, see Domozych, 1984). Because of their distinctive shape and intricate substructure, specific information concerning the precise morphological aspects of GA-mediated processing of individual scale types has been gathered for some forms (Moestrup and Walne, 1979). However, little if anything is known about the chemistry of the various scale types or the biochemistry of the unique secretory system involved in scale ontogenesis.

Recently, attempts have been made to elucidate the chemical nature of flagellar membrane scales and thecal scale components in thecate, green algal flagellates, close relatives of prasinophycean forms (Becker *et al.* 1989, 1990). These studies have reported distinct 2-keto-sugar acid-containing polysaccharides and distinct protein components. As part of an ongoing study of the secretory network in scale-bearing green algae, an analysis of the large, outer body scales of the freshwater prasinophyte, *Mesostigma viride*, was undertaken. This report describes structural and chemical analyses of the distinct basket scales.

Journal of Cell Science 100, 397–407 (1991)

Materials and methods

General and electron-microscopic analyses

Cultures of *Mesostigma viride* (CCAP 50/1) were routinely maintained in sterile Woods Hole medium (Nichols, 1973) enriched with soil extract (9 parts Woods Hole medium to 1 part soil extract) in 250 ml sterile Erlenmyer flasks in a Sherer Growth chamber (14/10 light–dark cycle, 2000 lux cool white fluorescent light, 17(±1)°C). Transfers were made every 2 weeks. For mass cultures, *Mesostigma* cultures were maintained in sterile, 15 l glass containers under the above conditions. Sterile air was pumped into the culture solution to maintain suspension agitation.

Cells were processed for routine transmission electron microscopy (TEM) using previously described techniques (Domozych, 1987). For immunocytochemistry, cells were fixed at 4 °C for 30 min in 0.5 % glutaraldehyde in 0.05 M cacodylate buffer (pH 7.8). Cells were then washed with cold (4 °C) cacodylate buffer three times by gentle resuspension and centrifugation. Cells were then pelleted into the tip of a cold beem capsule. Immediately thereafter, cells were sequentially dehydrated to 70 % ethanol in 10 % increments (10 min/increment) at 4 °C. After 10 min in 70 % ethanol, the beems capsules were brought to −20 °C in a cold box as described by Wells (1985). Dehydration then continued in 10 % increments (20 min/increment) to 100 % ethanol. Beem capsules with cells were then sequentially infiltrated with 10 %, 20 %, 30 %, 50 %, 60 %, 75 %, 90 % and 100 % London resin (LR White, Medium Grade; Agar Aids, UK) in an ethanol series (2 h per infiltration stage). The London resin was prepared with an ultraviolet (UV) accelerator (0.5 % benzoin methyl ether). Beem capsules were then left overnight at −20 °C in 100 % London resin. After a fresh change of London resin the next morning, the beem capsule–cell preparations were hardened by 24 h of indirect UV light treatment at −20 °C followed by an additional indirect UV polymerization at room temperature for an additional 24 h.

Antimonate labeling preparations and subsequent control EGTA digestion analyses were performed by the method of Wick and Hepler (1980). In addition, dissolution of antimonate precipitates in sections with 200 mM CDTA (trans-1,2-diaminocyclohexane-*N*,*N*,*N*′,*N*′-tetraacetic acid) was also undertaken.

For all TEM preparations, sections were cut using a Reichert Ultratome ultramicrotome and viewed on a JEOL 1200 EX TEM at 80 kV. For routine analyses, sections were stained with standard uranyl acetate/lead citrate prior to TEM viewing.

Basket scale isolation

Basket scale isolation was performed as follows: cells from mass cultures were harvested using a Sorvall continuous-flow centrifugation device (type KSB Szent-Gyorgiyi and Blum) attached to an RC-1 centrifuge. Wet cell pellets were resuspended with and washed several times with 50 mM Tris–HCl buffer (pH 7.8). Washed cell pellets were obtained *via* centrifugation at 2500 ***g*** in a Sorvall RC-2B centrifuge with an SS-34 rotor. After 3 washes, the cell pellet was resuspended in ice-cold 50 mM Tris–HCl buffer and sonicated to cavitation for 3, 1-min bursts using a Bransonic sonicator. Resultant cell suspensions were then contrifuged at 2500 ***g*** for 5 min. The supernatant, containing the basket scales, was recentrifuged at 27 000 ***g*** for 15 min. The resultant pellet, containing the basket scales, was resuspended in cold Tris buffer with 0.15 % Triton X-100 and sonicated as above. The suspension was recentrifuged at 27 000 ***g*** for 15 min. The pellet was resuspended/washed in ice-cold Tris buffer and recentrifuged 3 times. The resultant pellet was resuspended in 5 ml of Tris buffer and layered upon a discontinuous sucrose gradient cushion of 10 ml of 10 % sucrose/Tris, 5 ml of 20 % sucrose/Tris and 5 ml of 30 % sucrose/Tris. The gradient tube was centrifuged at 6000 revs min^{-1} for 15 min in an HS 133B swinging bucket rotor on a RC-2B centrifuge. A pure white layer in the middle of the 20 % sucrose layer was found to contain pure basket scales. This layer was carefully pipetted off, repeatedly washed with Tris buffer and finally distilled water (or dialyzed overnight with 9 l of cold distilled water). The resultant scale suspension was centrifuged at 27 000 ***g*** as above. The pellet was frozen in liquid N_2 and stored at −80 °C or freeze dried. For electron microscope analysis of purity, scales were pelleted down into Beem capsules, fixed with 1 % OsO_4/0.05 M cacodylate buffer (pH 7.8), dehydrated in acetone and infiltrated and embedded with Spurr's resin. Sectioning and TEM observation were performed as above. In some instances, scales were dried on a Formvar-coated/carbon-stabilized copper grid and rotary shadowed.

Biochemical and dissolution analyses

Scales were processed for electrophoresis by previously described methods (Hames, 1981). Scales were partially dissolved by boiling for 3 min in 0.0625 M Tris–HCl (pH 6.8), 2 % SDS, 5 % 2-mercaptoethanol, 10 % glycerol and 0.002 % Bromophenol Blue. Digested scale components were separated on a 5 % to 15 % polyacrylamide gel with a discontinuous buffer system. Total carbohydrate determination was by the method of Kochert (1978*a*) and total protein determination was by the method of Kochert (1978*b*). For scale dissolution analyses, a solution of 1 mg ml^{-1} of scales in distilled water was prepared, separated into 0.2 ml aliquots in 1.5 ml centrifuge tubes and centrifuged in a microcentrifuge. The resultant scale pellets were resuspended in: 0.1 M EDTA, 0.1 M EGTA, 200 mM CDTA, 2M KOH, 1M HCl, 1 % SDS, 67 % H_2SO_4, 0.5 M boric acid, 4 M urea, 2 M sodium perchlorate or distilled water. For room temperature studies, tubes were kept at 25 °C for 1–2 h or placed in a boiling water bath for 5 min or for EGTA and CDTA, placed in a 60 °C oven for 2 h. After treatments, the individual tubes were centrifuged and pellets (if present) were washed with 50 mM Tris–HCl buffer and recentrifuged. Suspensions of resultant pellets were processed and used for TEM and immunoblot analyses as described elsewhere in this study. When no pellet was visible, it was assumed that the scales were digested.

A carbohydrate analysis of the scales was performed at the Complex Carbohydrate Research Center (Athens, Georgia, USA). For glycosyl composition and linkage analysis, two methods were used: trimethylsilyl (TMS) methylglycoside analysis (for identification of acidic sugars, amino sugars and neutral sugars) and alditol acetate analysis (for neutral sugars) (York *et al.* 1985). The preparation of TMS methylglycosides was accomplished by dissolving the sample in 1 M HCl in methanol at 100 °C for 18 h. The solvents were evaporated, the sample was then *N*-acetylated using pyridine/acetic anhydride in methanol. The solvents were then again evaporated. The sample was then reacted with Tri-Sil reagent (Pierce Chem.) at 80 °C for 20 min. The solvents were then evaporated and the samples were dissolved in hexane and analyzed by gas chromatography (GC) and GC/mass spectral analysis (MS). Alditol acetates were prepared by hydrolyzing the sample in 2 M trifluoroacetic acid (TFA) at 120 °C for 2 h. Solvents were evaporated. The sample was reduced with sodium borodeuteride in acetic acid. Borate was removed by repeated evaporations with methanol/acetic acid. The sample was then acetylated with acetic anhydride in pyridine. The solvents were again evaporated. The alditol acetates were extracted with chloroform/water. The solvent was again evaporated, and the sample was dissolved with acetone and analyzed by GC and by GC/MS. Glycosyl linkage analysis was performed by methylation analysis. The sample was dissolved in dimethyl sulfoxide (DMSO). DMSO anion was added and the sample was stirred for 4 h. After this time, an excess of methyl iodide was added to this sample, which was stirred at room temperature overnight. The excess methyl iodide was evaporated. The permethylated sample was purified by C-18 Sep-Pak cartridge. The sample was then carboxyl-reduced with triethyl lithium borodeuteride. This was done in order to identify the linkages of any possible uronic acid residues. After triethyl lithium borodeuteride reduction, the sample was hydrolyzed in 2 M TFA, reduced with sodium borodeuteride, and acetylated as described above for the alditol acetate procedure. The resulting partially methylated alditol acetates were analyzed by GC and by GC/MS.

X-ray and FTIR (Fourier Transform Infrared Spectroscopy) analyses

For X-ray analysis, several techniques were employed: (1) scales were resuspended in distilled water (0.1 mg ml^{-1}) and drops were

placed onto 0.2% Formvar-coated/carbon-stabilized grids or onto carbon-based stubs with a carbon-based cement. The scale solution was allowed to stand for 5 min and excess water was drawn off by capillary action using Whatman no. 1 filter paper. After an additional 1 h of drying in a dust-free chamber these preparations were used for either SEM or STEM–X-ray analysis. For SEM X-ray analysis, the stubs with dried scales were analyzed with a Philips 501B scanning electron microscope fitted with a Link System 800 series 2 energy dispersive X-ray microanalysis system. An elemental spectrum was collected using the analysis program. The microscope was operated at 15 kV with the spot size adjusted to give approximately 300 counts s^{-1} for a live time of 100 s. STEM–X-ray analysis of grids with dried scales was performed with JEOL 1200 EX TEM equipped with an Tracor Northern X-ray Analyzer system. (2) The second method employed analysis of scales on cells fixed and embedded in plastic resin (see above). Fixation of cells did not include post-fixation with OsO_4. Gold sections (~150 nm) were cut and placed on Formvar-coated grids (see above). STEM–X-ray analysis was performed as above. Sections were not stained before being analyzed. In order to standardize the analysis for calcium and phosphorous, a 1% suspension of $CaHPO_4$ was made, and the particles were centrifuged down into the tip of a beem capsule. The pellet was then dehydrated and processed for plastic embedding as described above. Sections of this material were also analyzed by STEM–X-ray analysis. FTIR analysis of scales was obtained using a Digilab FTS-60 FTIR spectrometer (IR source of tungsten carbide with power of 110 milliwatts; single mode He–Ne laser; detector was a deuterated triglycerine sulfate (DTGS) pyroelectric detector with spectral range of 4400–450 cm^{-1}).

Immunological analyses

For immunological work, scales were suspended in complete Freund's adjuvant (200 $\mu g\,ml^{-1}$) and administered to 6-week-old, female Lou C rats. Two subsequent boosters were given at 3-week intervals. Blood samples were removed from the tail vein one week after the booster injections and centrifuged. The whole serum was used as the source of polyclonal antibody. Immunoblot analysis was performed as described by Smith *et al.* (1984). Immunofluorescence and immunocytochemistry studies were performed as described by Grief and Shaw (1987). For immunofluorescence studies, specimens were counter-stained for DNA with 4,6-diamidino-2-phenylindole (DAPI) and mounted in antifade mountant (Citifluor, London). For routine light microscopy (LM), cells were observed with a Zeiss universal microscope equipped with fluorescence optics. Confocal laser scanning microscopy was performed with a BIORAD MRC500 confocal laser scanning head attached to a Zeiss universal microscope. Computer-controlled fine-focusing of the microscope permitted the collection of focal section stacks. For further processing and analysis, the data sets were transferred to a Stardent Titan graphics workstation *via* an Ethernet link. The computer was used for interactive display of section stacks and calculation of projections of data sets and images were photographed from the display screen.

Results

Cell and scale morphology

Mesostigma viride is an unusual, biflagellated, unicellular green alga. The flattened cells (7–10 μm in length) possess a distinct central pit through which the two flagella emerge (Fig. 1A). An elongate chloroplast is narrowly appressed against the plasma membrane in the cell's posterior region. In one lobe of cytoplasm, delimited by the pit, is the nucleus. A scale-producing Golgi apparatus is usually situated in the other lobe of cytoplasm. Further details of basic cell ultrastructure have been published (Manton and Ettl, 1965). The cellular and flagellar surfaces of *Mesostigma* are covered by layers of distinctly shaped scales. The plasma membrane is coated with an inner layer of small rhomboid scales (30 nm), a medial stratum of naviculoid scales (200 nm by 300 nm), and an outer layer of highly elaborate, 'basket' scales (Fig. 1B). The basket scale is approximately 450–500 nm in height and 470 nm at its greatest width. This scale type consists of a solid base to which is connected an upwardly extending, latticed fibrillar network (Figs 1C, 2H, 3A). The squarish base consists of two rims, an outer and an inner. In the center of the base is a thick, fibrous lattice base that forms the foundation of the scale lattice work. Fibrillar struts anchor the lattice base to the corners of the rim of the base. The overall basket structure consists of two major sections: a lower basket lattice that forms the bulk of the scale and a thickened, upper lattice that sits upon the former lattice structure. The lower basket lattice contains an organized arrangement of fibers that create patterned fenestrations. Some of the fibers are thickened toward the basket interior to create a rib-like pattern (Fig. 2B and C). The basket is apparently supported by an external strut system of thickened fibers (Figs 1C,F and 2F,H). The strut

Fig. 1. (A) View of the basic overall ultrastructure of *Mesostigma viride*. The flattened cells are highlighted by a central depression, the pit (p) through which the two flagella emerge. The chloroplast (c) is found appressed to the plasma membrane in the posterior end of the cell. The nucleus (nu) occupies one lobe of the cytoplasm. The scaly extracellular matrix can be observed on the cell surface (arrowheads). This cell was prepared using routine TEM fixation. Bar, 1.0 μm. (B) Surface view of cell displaying the three types of scales. Upon the plasma membrane surface (pm) is an innermost layer of subrhomboid scales (1, arrowheads), a medial layer of oval scales (2, arrowheads) and the outermost layer of basket scales (3, arrowheads). The cell was fixed as in A. Bar, 500 nm. (C) Close-up view of a basket scale on fixed cell revealing most of the major components of scale architecture. The two scale lattices sit upon a solid base (b). The basket lattice structure (bl) emerges from the base and is supported by a branching strut system (s). The uppermost lattice, the rim lattice (rl), has two noticeable, thickened rims (r). Please see Fig. 3A and B. Bar, 100 nm. (D) Surface view of basket scale arrangement upon the surface of a fixed cell. Note the arrangement of scales in rough linear arrays that are slightly curved (arrowheads). Compare with Fig. 10A–D and 11A and B. bar, 500 nm. (E) View of isolated basket scales obtained *via* procedure outlined in Materials and methods. Note that the preparation is free of contamination from other scale types and cellular fragments. Bar, 1.0 μm. (F) Magnified view of isolated basket scale obtained as for E. Note the base (b), the basket lattice (bl), the supporting strut (s), the rim lattice (rl) and the thickened rims (r). This scale preparation was rotary shadowed (see Materials and methods). See also C and Fig. 3A and B for comparisons. Bar, 100 nm.

Fig. 2. (A–D) Serial cross-sections (125 nm thick) through a basket scale. (A) The top of two scales, highlighting the thick rims (r) and rim lattice (rl). (B) The same two scales at a lower level and displays the upper part of the basket lattice (bl) and basket lattice ribs (blr) extending into the central lumen. In C the lattice begins to narrow down and the basket lattice (bl) and basket lattice ribs (blr) are still observable. In D the base is highlighted. Note the flat base (b), the lattice base (lb) and the peripheral strut roots (sr). Bar, 200 nm. (E–J) Serial longitudinal sections (100 nm thick) through the basket scale. (E) Represents one end of the basket scale and highlights the rim lattice (rl) and upper rims (r). (F) Further into the scale, revealing the basket lattice (bl) and supporting strut roots (sr). (G and H) Approximately half-way through the scale, showing the basket lattice ribs (blr). (I) The basket lattice and scale roots at the other end of the scale. (L) Terminates the serial view by displaying the rim lattice (rl) on the other edge of the scale. Bar, 100 nm.

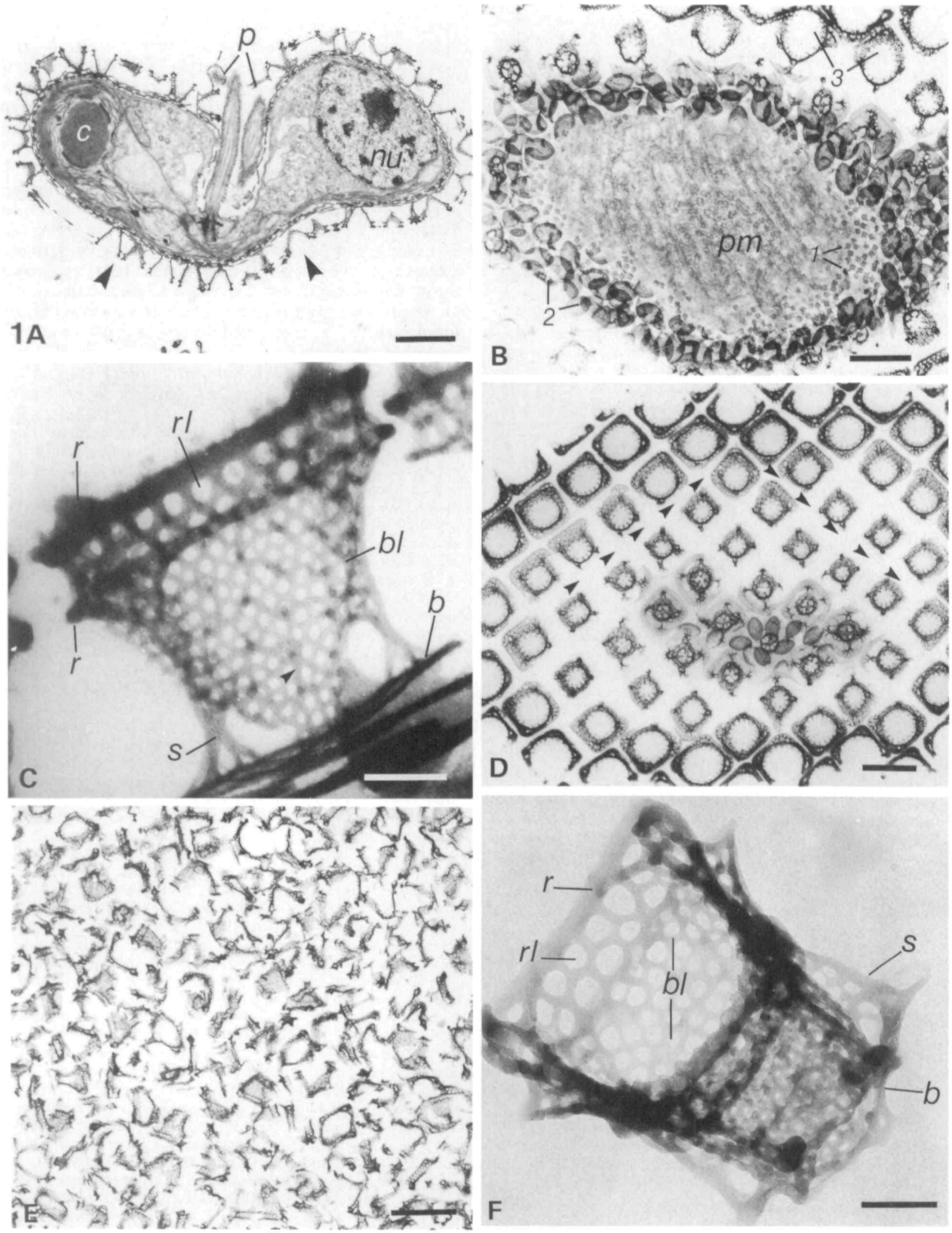

Fig. 1. For legend see p. 399

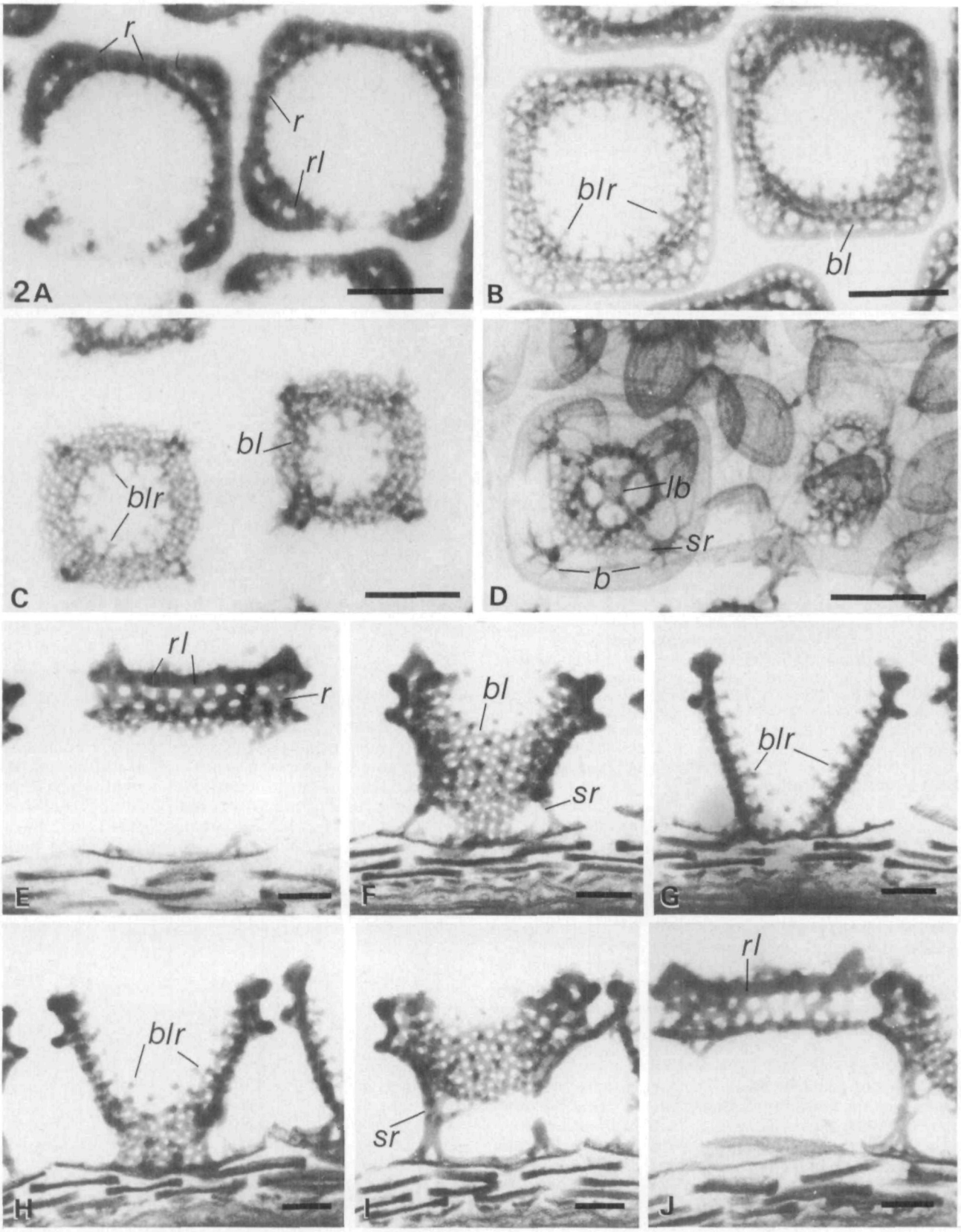

Fig. 2. For legend see p. 399

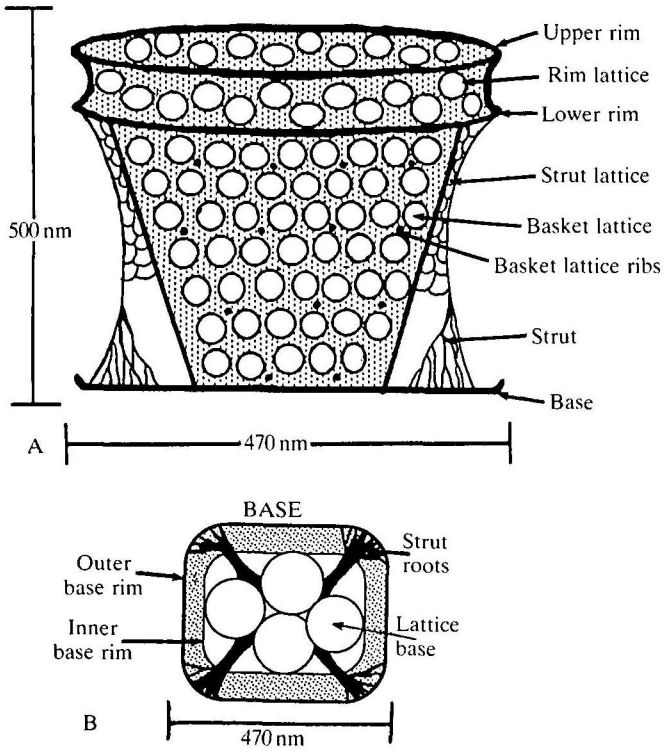

Fig. 3. Diagram of basket scale highlighting key architectural components. The scale is about 450–500 nm in height. The extensive latticular structure sits upon a squarish solid base of approximately 470 nm on a side. The basket lattice is highly fenestrated and has regular repeating, thickened ribs that extend inwards into the lumen. The basket lattice is supported by a strut system. The strut possesses a fibrillar lattice in regions just below the rim of the rim lattice and terminates on the base in root-like fibers. The upper portion of the scale contains a large lattice, the rim lattice, bordered by two thickened rims, the upper and lower. (B) Diagrammatic view of the scale base highlighting the outer and inner base rims, the basket lattice base and the strut roots.

terminates in a branched root system on the base (Figs 1C and 2D). The upper part of the strut also contains an inconspicuous, branching fibrillar network resulting in a strut lattice (data not shown). The upper lattice is delineated by upper and lower rims, both of which have a thickened fibrillar construction (Figs 1C, 2A,E and J). Thickened fibers are also organized between the rims and create a fenestrated rim lattice (Figs 1C, 2E,J). A model of the scale is presented in Fig. 3. Basket scales are closely packed on the cell surface, often resulting in somewhat distorted quasi-crystalline arrays (Fig. 1D).

Scale isolation and dissolution analysis

Basket scales could be easily removed from living cells employing the techniques outlined in Materials and methods. From a loose cell pellet obtained from centrifuging 10 l of active cell cultures (8 g wet weight), 10 mg of dried basket scales could be obtained. TEM analysis of isolated scales revealed no observable contamination with other scale types or cytoplasmic constituents (Fig. 1E). More importantly, isolated basket scales retained the typical form, indistinguishable from that observed upon cells (Figs 1F, 4A). Scale dissolution studies showed that scales were not digested when incubated in 0.1 M EGTA (60 °C, 2 h), 0.1 M EDTA (60 °C, 2 h), 0.5 M boric acid, 2 % SDS, 4 M urea or 2 M perchlorate at room temperature or at

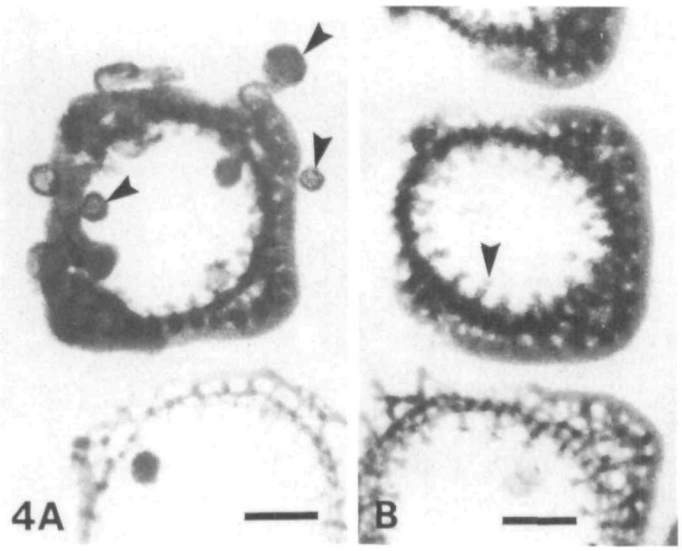

Fig. 4. (A–B) Views of a basket scale after labeling with antimonate (see Materials and methods). (A) The typical heavy labeling (arrowheads) on scales, especially that found upon the rims. When these scales are treated with 0.1 M CDTA for 2 h at room temperature, the antimonate precipitates are dissolved (see B). Bars, 100 nm.

100 °C. Scales were digested when treated with 67 % H_2SO_4, 1 M HCl, 2 mM CDTA, 2 M KOH or 1 % oxalic acid even at room temperature. Partial dissolution of scales occurred when scales were incubated in 0.5–1.0 M acetic acid at high temperatures; here the scales were transformed into an unorganized mass of fibrillar material.

X-ray and FTIR analyses

Isolated basket scales were analyzed by X-ray microanalysis to determine elemental composition. SEM–X-ray analysis of dried scales on a carbon SEM stub revealed two distinct peaks, a calcium peak and a smaller phosphorus peak (Fig. 5). This result was confirmed by STEM–X-ray microanalysis of scales dried upon a copper grid. Likewise, STEM–X-ray microanalysis of scales from gold sections of fixed and plastic-embedded cells revealed distinct calcium

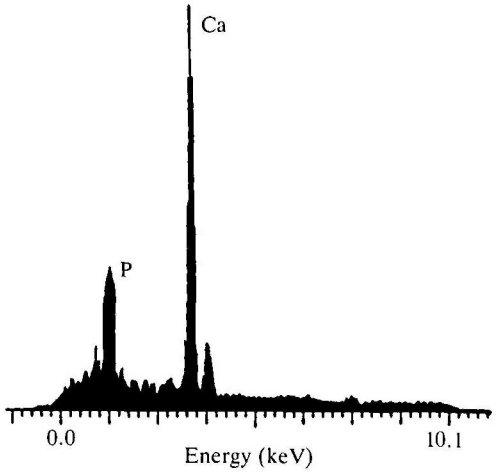

Fig. 5. SEM–X-ray EDS spectrum of basket scales placed on carbon-coated stub. Note that the two dominant elements found in the scales are calcium and phosphorus. Note also that both the kα and kβ peaks of calcium are detected.

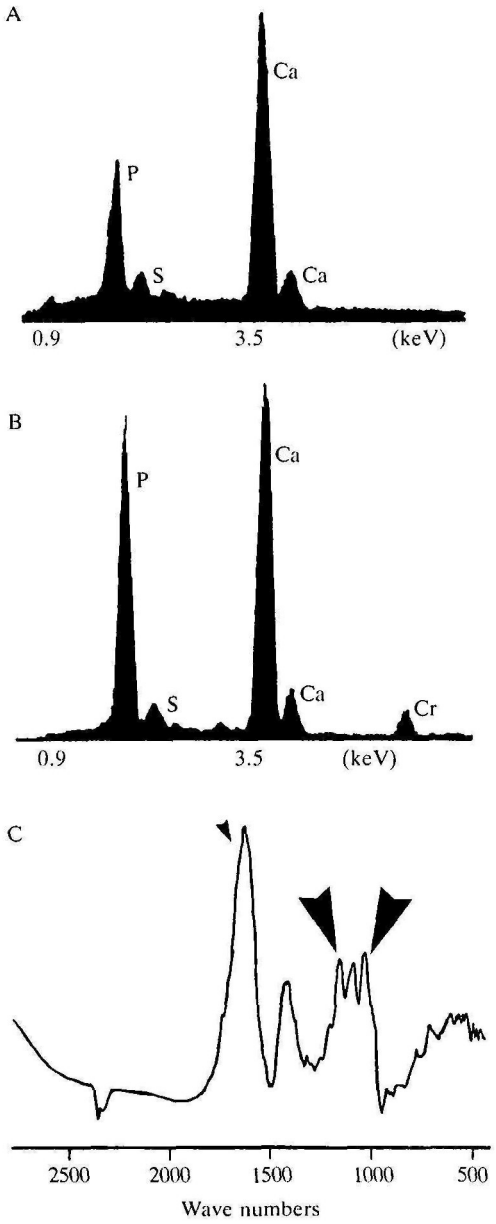

Fig. 6. (A) STEM–X-ray spectrum of a section (150 nm) of a basket scale embedded in plastic (see Materials and methods). Note that both calcium (kα and kβ peaks) and phosphorus are the dominant elements identified. A small amount of sulfur was also noted. (B) STEM–X-ray spectrum of a $CaHPO_4$ standard embedded in plastic. This control spectrum displays a similar spectrum to that obtained for the basket scales (see A). (C) FTIR spectrum of isolated basket scales. The tri-peaks at 1156, 1086 and 1024 (large arrowheads) indicate the presence of a phosphate group (asymmetric stretch). The large peak at 1625 indicates the presence of -OH, probably as water.

and phosphorus peaks (Fig. 6A). Analysis of the $CaHPO_4$ particle standards in plastic sections revealed similar and distinct calcium and phosphorus peaks (Fig. 6B). In all sectioned materials, X-ray analysis of cellular parts other than basket scales, as well as non-cellular plastic areas, never revealed the presence of calcium or phosphorus. In all X-ray preparations, both kα and kβ peaks of calcium were observed.

In order to supplement the X-ray studies of the mineral

Fig. 7. SDS–gel electrophoresis of isolated basket scales in 5% to 15% acrylamide gradient gel and stained with Coomassie Blue. Lane A represents scales digested for 1 min and lane B represents scales digested for 3 min before application to gels (see Materials and methods). Two distinct bands are noticeable, one that remains at the origin (1, arrowhead) and a second (2, arrowhead) with an estimated M_r of about 48 000. Periodic acid–Schift (PAS) staining did not stain these bands nor did it reveal other bands.

content of scales, whole cells were fixed and processed for TEM without osmication (or other staining) and labeled with antimonate using the method of Wick and Hepler (1980). When observed with the TEM, antimonate labeling was highly localized on the basket scales (Fig. 4A). When antimonate-labeled sections were treated with 0.1 M EGTA for 2 h at 60°C or with 0.1 M CDTA for 2 h at room temperature, antimonate precipitates were removed (Fig. 4B). These results also indicate the presence of a cation like calcium, complexed to the scales. FTIR spectral analysis of basket scales was also performed to elucidate further the chemical nature of the scales (Fig. 6C). This analysis revealed distinct peaks at 1156, 1086 and 1024 cm^{-1}, indicating the presence of a phosphate group (asymmetric stretch).

Biochemical analyses

Biochemical analyses revealed that isolated scales consisted of 24% carbohydrate and 5% protein. SDS–gel electrophoresis of partially dissolved scales revealed two noticeable bands (Fig. 7), one migrating band with an approximate relative molecular mass of 48 000 and one band that did not migrate into the gel; 16.5% of the total scale mass (or 68%) of the total carbohydrates was identified as glucose. GC-MS analyses of TMS glycosides derived from basket scales revealed only two major sugars (Fig. 8). Neither galacturonic acid, glucuronic acid nor any amino sugars could be identified in the TMS glycoside procedure. However, there were two peaks in which the mass spectra indicated there were sugar residues. These peaks had a characteristic fragment ion, m/z 204, which is indicative of a pyranose sugar residue. The two major unknown peaks were shown to have identical mass spectra to the methyl glycosides of the pyranose and furanose forms of the sugar, 3-deoxy-lyxo-2-heptulosaric acid or DHA. The ratio of DHA to glucose from the GC area analysis was estimated to be 0.63.

Immunological analyses

Basket scales proved to be highly antigenic and the

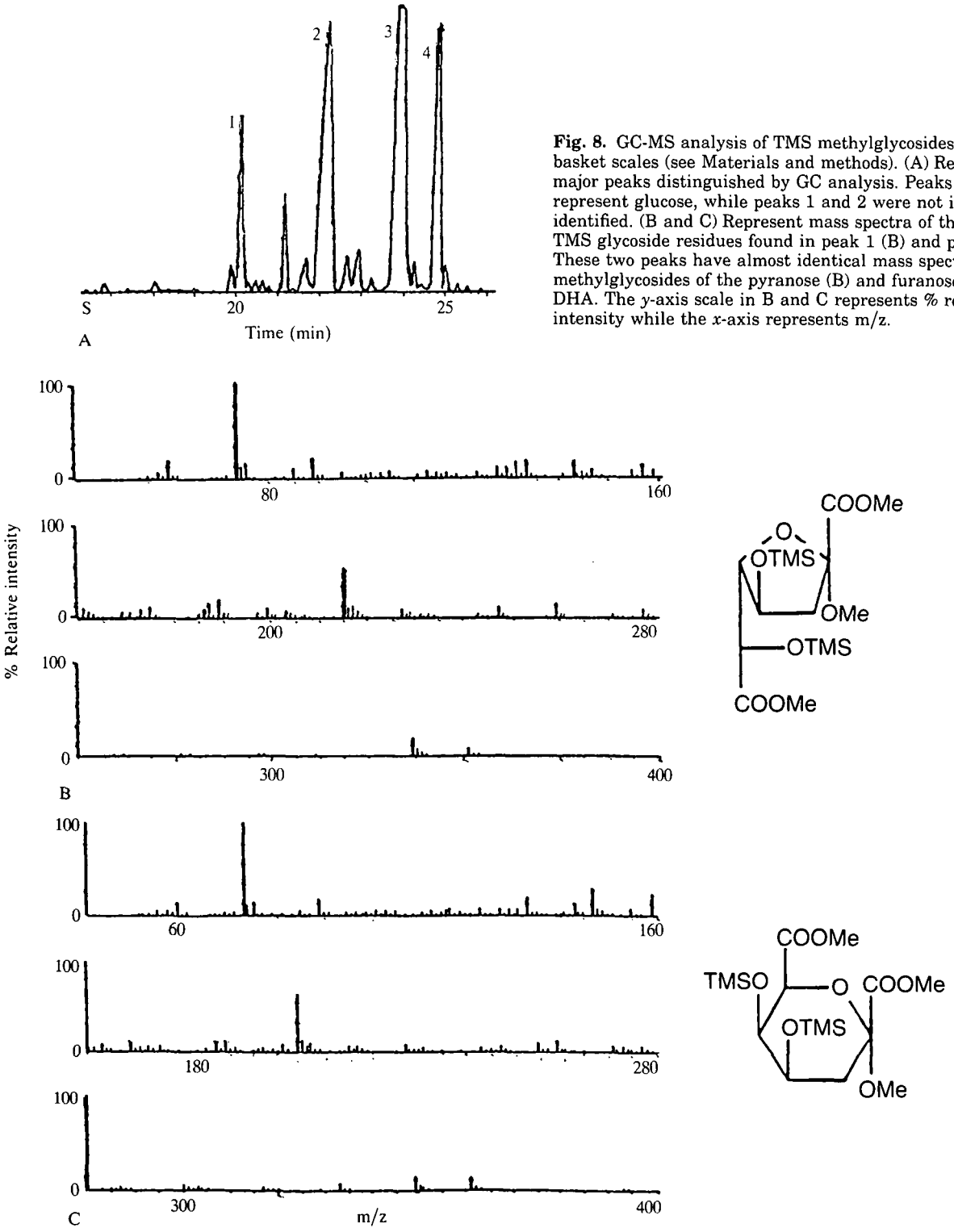

Fig. 8. GC-MS analysis of TMS methylglycosides derived from basket scales (see Materials and methods). (A) Represents the major peaks distinguished by GC analysis. Peaks 3 and 4 represent glucose, while peaks 1 and 2 were not immediately identified. (B and C) Represent mass spectra of the GC-separated TMS glycoside residues found in peak 1 (B) and peak 2 (C). These two peaks have almost identical mass spectra to the TMS methylglycosides of the pyranose (B) and furanose (C) forms of DHA. The *y*-axis scale in B and C represents % relative intensity while the *x*-axis represents m/z.

polyclonal antibody obtained from rat proved to be very useful in chemical and immunocytochemical analyses of the basket scales. In immunoblot analyses, the antibody reacted very strongly and specifically to the basket scales (Fig. 9A). Scales that were treated under various chemical conditions were also analyzed immunologically (Fig. 9B). Only treatment of scales with 2 M periodate destroyed the antibody binding. This result suggested that the antibody was specific for a sugar moiety of the scale. Immuno-gold labeling of the scales using the isolated antibody revealed specific binding to the basket scales (Fig. 9C and D), at the basket lattice and strut fibers.

Immunofluorescence analyses of whole cells highlighted the scales and their patterning on the cell surface (Fig. 10A–C). Studies using conventional fluorescence microscopy and confocal laser scanning microscopy followed by three-dimensional projection revealed that the scales were in a close-packed arrangement resulting in

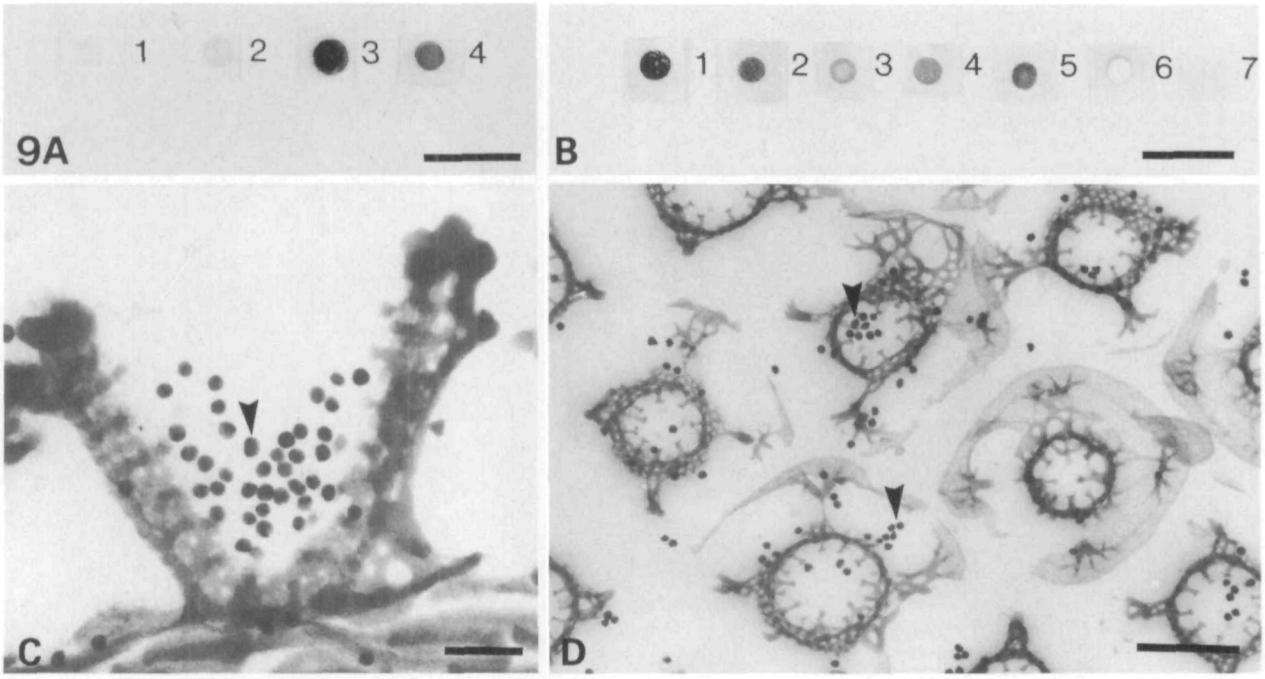

Fig. 9. Immunoblot analysis (see Materials and methods) of antibody raised against basket scales in female Lou C rats. Lane 1, control, no primary antibody applied to nitrocellulose sheets; lane 2, control, no scales applied to nitrocellulose sheet; lane 3, strong reaction of antibody–scale complex; lane 4, antibody–scale complex as in lane 3 with only half the amount of scale material added to nitrocellulose sheet. Bar, 0.5 cm. (B) Immunoblot analysis of scales treated with various chemical agents. Lane 1, normal antibody–scale complex; lane 2, scales treated with 0.1 M EGTA (60 °C, 2 h); lane 3, scales treated with 2 % SDS; lane 4, scales treated with 0.1 M EDTA (60 °C, 2 h); lane 5, scales treated with 4 M urea; lane 6, scales treated with 2 M perchlorate; lane 7, control, no primary antibody. Bar, 0.5 cm. (C–D) Immunogold labeling of basket scales using with isolated rat antibody. Note the specific labeling of basket scales (arrowheads), especially at the lattice areas. The base components do not label as intensely as the lattices. Bars: 100 nm (C); 200 nm (D).

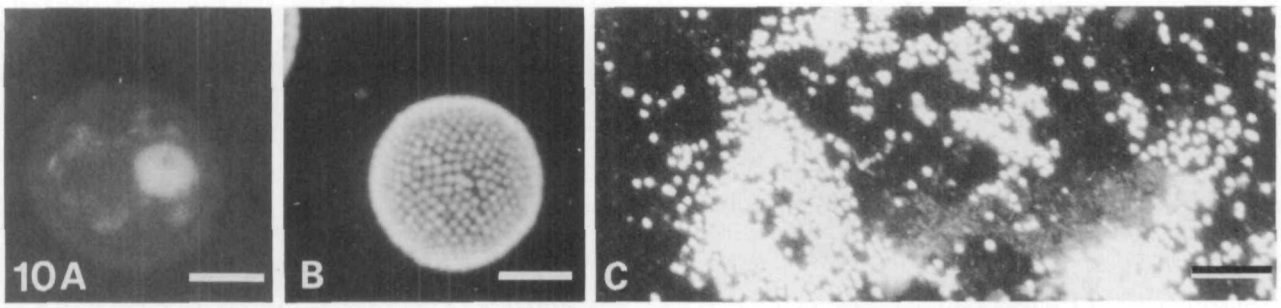

Fig. 10. (A–C) Immunofluorescence analysis of *Mesotigma* basket scales (see Materials and methods). (A) Highlights DAPI staining of immunolabeled cell. (B) Represents cell from A labeled with scale antibody. Note the individual scales upon the cell surface. (C) Represents a crushed cell labeled with scale antibody. Individual fluorescent scales released into the slide medium can easily be seen. Bar, 3.2 μm.

quasi-crystalline arrays upon the plasma membrane surface (Figs 10 and 11). These arrays tended to curve upon the cell surface. These data permitted an estimate of the number of basket scales to be made: it was estimated that a cell of 8 μm in length contained approximately 800 basket scales.

Discussion

The basket scale of *Mesostigma* is a highly elaborate structure consisting of an intricately interwoven series of thin and thick fibers. The results from our X-ray and FTIR analyses show that the basket scales are mineralized extracellular coverings. The high degree of order seen in scale fiber arrangement which is manifest in the overall elaborate microarchitecture of the basket scale does indeed suggest a mineralized system. The dominant elements in the scale complex are calcium and phosphorus, possibly organized in a calcium–phosphate complex. This report presents evidence for the first time that a body scale of a prasinophyte is, in fact, mineralized. Little or no evidence previously existed suggesting that true prasinophycean scales contained significant amounts of calcium or other minerals. In fact, it was previously thought that the scales were non-mineralized entities

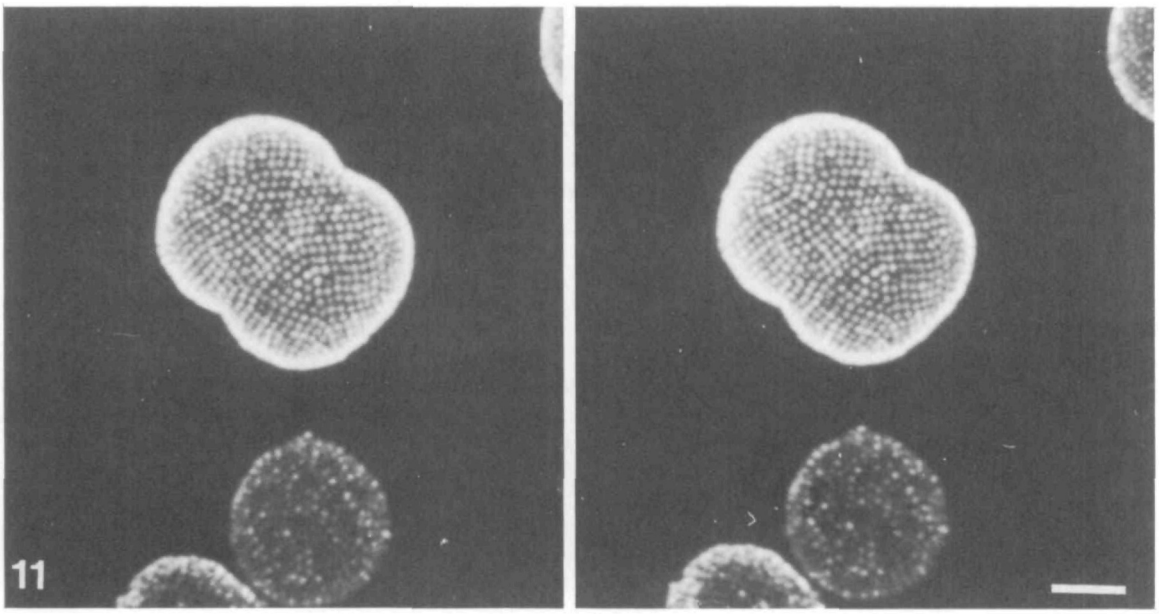

Fig. 11. Stereo view of basket scale arrangement on the cell surface as highlighted by immunofluorescence and confocal laser scanning microscopy. The scales are positioned upon the cell surface in a close-packed fashion resulting in quasi-crystalline arrays. Bar, 3 μm.

(Moestrup and Walne, 1979). Recently, reports have shown that the scale-like entities of the thecae of pleurastrophycean (sensu Mattox and Stewart, 1984) flagellates do contain calcium and that calcium may maintain scale integrity and scale–scale interactions (Melkonian *et al.* 1986). It will be of interest to ascertain the distribution of mineralized scales in the parasinophycean taxon.

The evidence presented here suggesting the possible existence of a calcium–phosphate mineralized scale is quite intriguing for this would represent a novel mineral type in the extracellular covering of green algae. Only calcium carbonate and calcium oxalate complexes have been previously recorded in green algae (Simkiss and Wilbur, 1989). Similarly, calcium phosphate mineralized systems are more characteristic of higher animals, particularly in components of their skeletal systems. It is important to note that definite confirmation of a calcium–phosphate complex as well as identification of the type of crystalline form of calcium phosphate remains to be elucidated. It is also possible that the calcium and phosphate may be parts of two different mineralized systems within the basket scale. It is a common occurence in some biological systems that the formation of one mineralized complex may also provide a surface for the nucleation of another salt. For example, the common occurrence of calcium and carbonate ions in many biological systems has led to the suggestion that calcium carbonate may be a ubiquitous solid phase upon which other minerals grow (Nancollas *et al.* 1983). In the Mesostigma basket scale complex it is possible that calcium carbonate is initially complexed to an organic matrix (see below), and that later phosphate precipitates are deposited on this initial complex. Further work needs to be done to elucidate the substructure of the calcium–phosphate association as well as the processing steps by which these minerals are added on to the growing scale.

The discovery of the 2-keto-sugar acid, DHA, in the scale was also most interesting. This uncommon sugar has been found in the rhamnogalacturonan II component of cell walls of various angiosperms and gymnosperms and, more recently, in the scale components of the thecate green alga, *Tetraselmis* (Becker *et al.* 1989, 1990). Work is presently under way in this laboratory to determine the precise nature of the DHA linkages and the association of this acidic sugar with the rest of the polysaccharide moiety. It will be of interest to see if this sugar is found in the scales of other prasinophytes and whether its distribution could be used as a diagnostic feature in taxonomic studies of prasinophytes. Likewise, it will be significant to determine the evolutionary distribution of DHA in advanced green algae and higher plants. More importantly, it will be of interest to note if this acidic sugar is the negatively charged matrix material that is responsible for binding calcium and thus mediating the formation of the basket scale. If this is the case, it will be important to discover where this sugar is processed in the scale secretory network and how it contributes to scale formation. For example, a major question that needs to be answered is: does the addition of DHA to a neutral matrix in particular dictyosome cisternae trigger the complexing of calcium and formation of scales?

The arrangement of basket scales on *Mesostigma* is highly organized. The antibodies raised against the isolated scales in this study proved to be valuable tools in in identifying scales at the LM level and studying their surface distribution. The arrangement of the scales on the cell surface was found to be in a close-packed lattice that, in turn, created rough linear arrays. These arrays were slightly curved, perhaps due to the underlying contour of the cell or to the scale release mechanism upon the surface of the cells. Clearly, future use of similar immunofluorescence techniques will be important in elucidating the point of scale release from the cell, the actual patterning of scale release and quantitative aspects of scale production.

Many questions remain to be answered about the basket scales of *Mesostigma*. How are the scales maintained upon the surface, for they are not directly attached to the plasmamembrane but onto other underlying scales? How

are scales processed within the various compartments of the dictyosome? Are scale production and release coordinated with cellular cycles? Finally, what are the specific functions of scales? Answers to these questions will provide valuable insight into the function of the endomembrane system and cell surface interactions in primitive green plants as well as information elucidating the evolution of the cell wall in green algae.

The authors thank Dr Martin W. Steer, Barry Cregg and Shea Giles (University College, Dublin, Ireland) for use of the STEM–X-ray unit; A. J. Quinn and S. Bennett of the Schools of Environmental Sciences and Chemical Sciences of the University of East Anglia (Norwich, England); S. A. Clarke and P. S. Belton of the AFRC Institute of Food Research (Norwich, England) for the SEM X-ray and FTIR analyses; and Russell W. Carlson of the Complex Carbohydrate Research Center of the University of Georgia for the biochemical analyses. This work was supported by a Cottrell College Research Grant (Research Corporation Grant). This work performed at the University of Georgia was supported in part by the USDA/DOE/NSF Plant Science Centers program; this particular grant has been funded by the Department of Energy grant DE-FG09–87-ER13810. Also, the authors thank Jan Peart and Christine Cooper of the Department of Cell Biology of the John Innes Institute for their assistance in obtaining antibodies, and Alison Bevin for all of her help during the course of this work.

References

ADAIR, W. S. AND SNELL, W. J. (1990). The Chlamydomonas reinhardtii cell wall: Structure, biochemistry, and molecular biology. In *Organization and Assembly of Plant and Animal Extracellular Matrix* (ed. W. S. Adair and R. P. Mecham), pp. 15–84. New York: Academic Press.

ALI, M. S., MITSUI, T. AND AKAZAWA, T. (1986). Golgi-specific localization of transglycosylases engaged in glycoprotein biosynthesis in suspension-cultured cells of sycamore (*Acer pseudoplatanus* L.). *Archs Biochem. Biophys.* **251**, 421–431.

BECKER, B., HARD, K., MELKONIAN, M., KAMMERLING, J. P. AND VLIEGENTHART, J. F. G. (1989). Identification of 3-deoxy-manno-2-octulosonic acid, 3-deoxy-5-O-methyl-manno-2-octulosonic acid and 3-deoxy-lyxo-2-heptulosaric acid in the cell wall (theca) of the green alga, *Tetraselmis striata* Butcher (Prasinophyceae). *Eur. J. Biochem.* **182**, 153–160.

BECKER, D., BECKER, B., SATIR, P. AND MELKONIAN, M. (1990). Isolation, purification and characterization of flagellar scales from the green flagellate *Tetraselmis striata* (Prasinophyceae). *Protoplasma* **156**, 103–112.

BRUMMELL, D. A., CAMIRAND, A. AND MACLACHLAN, G. A. (1990). Differential distribution of xyloglucan glycosyl transferases in pea Golgi dictyosomes and secretory vesicles. *J. Cell Sci.* **96**, 705–710.

DOMOZYCH, D. S. (1984). Cytokinesis, wall development, and morphogenesis in green algal flagellates, In *Structure, Function and Biosynthesis of Plant Cell Walls* (ed. W. M. Dugger and S. Bartnicki-Garcia), pp. 235–255. Baltimore: Waverly Press.

DOMOZYCH, D. S. (1987). Cell division in *Carteria crucifa* (Chlorophyta). The role of the endomembrane system and phycoplast. *Protoplasma* **136**, 170–182.

DOMOZYCH, D. S. (1989). Scales, glycoproteins and cellulose. In *Cellulose and Wood. Chemistry and Technology* (ed. C. Schuerch), pp. 611–622. New York: Wiley and Sons.

GRIEF, C. AND SHAW, P. J. (1987). Assembly of cell-wall glycoproteins of *Chlamydomonas reinhardii*: Oligosaccharides are added in medial and trans Golgi compartments. *Planta* **171**, 302–312.

HAMES, B. D. (1981). An introduction to polyacrylamide gel electrophoresis. In *Gel Electrophresis of Proteins, a Practical Approach* (ed. B. D. Hames and D. Rickwood), pp. 1–91. Washington, DC: IRL Press.

KOCHERT, G. (1978*a*). Protein determination by dye binding. In *Handbook of Phycological Methods. Physiological and Biochemical Methods* (ed J. A. Hellebust and J. S. Craigie), pp. 91–93. Cambridge: Cambridge University Press.

KOCHERT, G. (1978*b*). Carbohydrate determination by the phenol-sulfuric acid method. In *Handbook of Phycological Methods. Physiological and Biochemical Methods* (ed. J. A. Hellebust and J. S. Craigie), pp. 95–97. Cambridge: Cambridge University Press.

MANTON, I. (1966). Observations on scale production in *Pyramimonas amylifera*. *J. Cell Sci.* **1**, 429–438.

MANTON, I. AND ETTL, H. (1965). Observations on the fine structure of *Mesotigma viride* Lauterborn. *J. Linn. Soc. (Bot.)* **59**, 175–184.

MATTOX, K. R. AND STEWART, K. D. (1984). Classification of the green algae: A concept based on comparative cytology. In *Systematics of Green Algae* (ed. D. E. G. Irvine and D. M. John), pp. 29–72. London: Academic Press.

MELKONIAN, M., MCFADDEN, G. I., REIZE, I. B. AND BECKER, D. (1986). Secretion of organic scales in green algae: Secretory products are transported through the Golgi Apparatus by cisternal progression. *Ber. dt. bot. Ges.* **99**, 263–280.

MOESTRUP, O. AND WALNE, P. L. (1979). Studies on scale morphogenesis in the Golgi apparatus of *Pyramimonas tetrarhynchus* (Prasinophyceae). *J. Cell Sci.* **36**, 437–459.

MOORE, P. J. AND STAEHELIN, L. A. (1988). Immunogold localization of the cell-wall-matrix polysaccharides rhamnogalacturonan I and xyloglucan during cell expansion and cytokinesis in *Trifolium pratense* L.: implication for secretory pathways. *Planta* **174**, 433–445.

MOORE, P. J., SWORDS, K. M. M., LYNCH, M. A. AND STAEHELIN, E. L. A. (1991). Spatial organization of the assembly pathways of glycoproteins and complex polysaccharides in the Golgi apparatus of plants. *J. Cell Biol.* **112**, 589–602.

NANCOLLAS, G. H., SAWADA, K. AND SCHRUTTRINGER, E. (1983). Mineralization reactions involving calcium carbonates and phosphates. In *Biomineralization and Biological Metal Accumulation* (ed. P. Westbroek and E. W. de Jong), pp. 155–169. D. Reidel, Dordecht.

NICHOLS, H. W. (1973). Growth media-freshwater. In *Handbook of Phycological Methods. Culture Methods and Growth Measurements*, vol. 1 (ed. J. R. Stein), pp. 7–24. Cambridge: Cambridge University Press.

NORRIS, R. E. (1980). Prasinophytes. In *Phytoflagellates* (ed. E. R. Cox), pp. 85–146. New York: Elsevier/North Holland.

PENNICK, N. C. (1984). Comparative ultrastructure and occurence of scales in Pyramimonas (Chlorophyta, Prasinophyceae). *Arch. Protistenk.* **128**, 3–11.

PORCELLA, R. A. AND WALNE, P. L. (1980). Microarchitecture and envelope development in *Dysmorphococcus globosus* (Phacotaceae, Chlorophyceae). *J. Phycol.* **16**, 280–290.

ROBERTS, K. (1989). The plant extracellular matrix. *Curr. Opin. Cell Biol.* **1**, 1020–1027.

ROBERTS, K., GRIEF, C., HILLS, G. J. AND SHAW, P. J. (1985). Cell wall glycoproteins: structure and function. *J. Cell Sci. Suppl. 2*, 105–127.

SIMKISS, K. AND WILBUR, K. M. (1989). *Biomineralization. Cell Biology and Mineral Deposition*, pp. 328. Academic Press, New York.

SMITH, E., ROBERTS, K., HUTCHINGS, A. AND GALFRE, G. (1984). Monoclonal antobodies to the major structural glycoprotein of the *Chlamydomonas*. *Planta* **16**, 330–338.

STAEHELIN, L. A. AND CHAPMAN, R. L. (1987). Secretion and membrane recycling in plant cells: novel intermediary structures visualized in ultrarapidly frozen sycamore and carrot suspension-culture cells. *Planta* **171**, 43–57.

STAEHELIN, L. A., GIDDINGS, T. H., KISS, J. Z. AND SACK, F. D. (1990). Macromolecular differentiation of Golgi stacks in root tips of *Arabidopsis* and *Nicotiana* seedlings as visualized in high pressure frozen and freeze-substituted samples. *Protoplasma* **157**, 75–91.

VARNER, J. E. AND LIN, L. S. (1989). Plant cell wall architecture. *Cell* **56**, 231–239.

WELLS, B. (1985). Low temperature box and tissue handling device for embedding biological tissue for immunolabelling in electron microscopy. *Micron Microsc. Acta* **16**, 49–53.

WICK, S. M. AND HEPLER, P. K. (1980). Localization of Ca^{2+}-containing antomonate precipitates during mitosis. *J. Cell Biol.* **86**, 500–513.

YORK, W. S., DARVILL, A. G., MCNEIL, M. AND ALBERSHEIM, P. (1985). 3-deoxy-D-manno-2-octulosonic acid is a component of rhamnogalacturonan II, a pectic polysaccharide in the primary walls of plants. *Carb. Res.* **130**, 109–126.

(Received 28 May 1991 – Accepted 12 July 1991)